Available online at www.sciencedirect.com
SCIENCE DIRECT
International Journal of Pharmaceutics 318 (2006) 28–40
INTERNATIONAL JOURNAL OF PHARMACEUTICS
www.elsevier.com/locate/ijpharm

Effects of the anti-neoplastic agent ET-18-*O*CH_3 and some analogs on the biophysical properties of model membranes

Alejandro Torrecillas [a], J. Daniel Aroca-Aguilar [a,1], Francisco J. Aranda [a], Consuelo Gajate [b,c], Faustino Mollinedo [b], Senena Corbalán-García [a], Ana de Godos [a], Juan C. Gómez-Fernández [a,*]

[a] *Departamento de Bioquímica y Biología Molecular "A", Facultad de Veterinaria, Universidad de Murcia, Apartado de Correos 4021, E-30080 Murcia, Spain*
[b] *Centro de Investigacíon del Cáncer, Instituto de Biología Molecular y Celular del Cáncer, Consejo Superior de Investigaciones Científicas (CSIC), Universidad de Salamanca, E-37007 Salamanca, Spain*
[c] *Unidad de Investigación, Hospital Universitario de Salamanca, E-37007 Salamanca, Spain*

Received 3 February 2006; received in revised form 8 March 2006; accepted 10 March 2006
Available online 17 March 2006

Abstract

The effect of 1-*O*-octadecyl-2-*O*-methyl-*sn*-glycero-3-phosphocholine (ET-18-*O*CH_3, edelfosine), and six other analog asymmetric phosholipids on the physical properties of 1,2-dimyristoyl-*sn*-glycero-3-phosphocholine (DMPC) model membranes was studied using differential scanning calorimetry (DSC), ^{31}P-nuclear magnetic resonance (^{31}P NMR) and X-ray diffraction. DSC data revealed that, at concentrations of 40 mol% and higher, a new type of mixtures with higher T_c and narrower transitions appeared with all the asymmetric lipids studied. At very high concentrations of these lipids (50–80 mol%), destabilization was observed in the systems probably because of the formation of micelles or small vesicles. In all cases, the asymmetric lipids at concentrations of 40 mol% induced the formation of interdigitated structures in the lamellar gel phase, as deduced from X-ray diffraction. The asymmetric phospholipids were also added to 1,2-dielaidoyl-*sn*-glycero-3-phosphoethanolamine (DEPE) model membranes and DSC data revealed that the lipids primarily affected transition from the lamellar gel (L_β) to the lamellar liquid crystalline (L_α) phase in two aspects: the transition temperature was reduced, and the transition itself became broader and smaller. The lamellar liquid crystalline (L_α) to inverted hexagonal phase (H_{II}) transition was also affected, as detected by DSC and ^{31}P NMR data. Increasing concentrations of the asymmetric lipids reduced the formation of inverted hexagonal phases, which were completely inhibited in the case of ET-18-*O*CH_3. Since these compounds have been shown to have important biological actions through the plasma membrane, these results may help to understand the mechanism of action of these compounds. In addition these asymmetric lipids were tested for their capacity to induce cell apoptosis, and only ET-18-*O*CH_3 was found to have a clear effect, thus suggesting that the apoptotic effect is not exerted through changes in the biophysical properties of model membranes.

Keywords: ET-18-*O*CH_3; ET-18-OH; ET-18-H; ET-16-*O*CH_3-Ser; PAPC; LPC; PAF; Model membranes; ^{31}P-NMR

Abbreviations: DEPE, 1,2-dieladoyl-*sn*-glycero-3-phosphoethanolamine; DMPC, 1,2-dimyristoyl-*sn*-glycero-3-phosphocholine; DSC, differential scanning calorimetry; EDTA, ethylenediaminetetraacetic acid; ET-16-*O*CH_3-Ser, 1-*O*-hexadecyl-2-*O*-methyl-*sn*-glycero-3-phosphocholine; ET-18-H, 1-*O*-octadecyl-*sn*-glycero-3-phosphocholine; ET-18-*O*CH_3, 1-*O*-octadecyl-2-*O*-methyl-*sn*-glycero-3-phosphocholine; ET-18-OH, 1-*O*-octadecyl-2-hydroxy-*sn*-glycero-3-phosphocholine; H_{II}, inverted hexagonal phase; L_α, lamellar liquid crystalline phase; LPC, 1-palmitoyl-2-hydroxy-*sn*-glycero-3-phosphocholine; LUVs, large unilamellar vesicles; $L_{\beta'}$, lamellar gel phase; $L_{\beta I}$, interdigitated gel phase; MLVs, multilamellar vesicles; MOPS, 3-[*N*-morpholine]propane sulfonic acid; PAF, platelet-activating factor; PAPC, 1-palmitoyl-2-acetyl-*sn*-glycero-3-phosphocholine; PE, phosphatidyl ethanolamine; PKC, protein kinase C; ^{31}P NMR, ^{31}P-nuclear magnetic resonance; T_c, transition temperature; $\Delta\sigma$, chemical shift anisotropy

* Corresponding author. Tel.: +34 968364766; fax: +34 968364766.
E-mail address: jcgomez@um.es (J.C. Gómez-Fernández).
[1] Present address: Área de Genética, Facultad de Medicina, Universidad de Castilla-La Mancha, Centro Regional de Investigaciones Biomédicas, Avenida de Almansa, s/n, E-02071 Albacete, Spain.

0378-5173/$ – see front matter © 2006 Elsevier B.V. All rights reserved.
doi:10.1016/j.ijpharm.2006.03.008

1. Introduction

Asymmetric phospholipids, such as 1-*O*-octadecyl-2-*O*-methyl-*sn*-glycero-3-phosphocholine (ET-18-*O*CH_3, edelfosine) and some structural analogs, constitute a heterogeneous group of synthetic compounds of high metabolic stability and with different biological effects, including the inhibition of tumor growth (Berdel et al., 1981a; Hayashi et al., 1985; Ngwenya et al., 1991; Brachwitz and Vollgraf, 1995; Gajate and Mollinedo, 2002) as well as the induction of cell differentiation (Paul et al., 1987; Hochhuth et al., 1990) and apoptosis (Mollinedo et al., 1993, 1997; Ruiter et al., 2003). Their ability to inhibit proliferation is well known, as it is effective with prostate cancer cells (Berdel et al., 1981b), different human and murine leukemic cell cytes (Berdel et al., 1983; Wierenga et al., 2000), human brain and lung tumors (Berdel et al., 1984; Denizot et al., 2001), and others (Houlihan et al., 1987; Kosano and Takatani, 1988; Haugland et al., 1999; Lu et al., 2002). It has recently been reported that these compounds can also inhibit the multiplication of the human immunodeficiency virus type I (HIV-I) (Kucera et al., 1990; Mavromoustakos et al., 2001).

Asymmetric ether lipids do not interfere directly with DNA and are not mutagenic (Mavromoustakos et al., 1996), unlike most anti-tumor agents. The mechanism used by these compounds to inhibit cell proliferation is not well known, probably because of the variety of ways in which they act, for example, in the cellular transport system (Hoffman et al., 1992; Besson et al., 1996), cytokine synthesis (Nasu et al., 1999; Lu et al., 2002), intracellular calcium level modulation (Lohmeyer et al., 1994) or the interaction with enzymes, most of them associated to membranes and involved in lipid metabolism (Vogler et al., 1985; Brachwitz and Vollgraf, 1995; Wieder et al., 1995; Van der Luit et al., 2002) and/or in signaling transducing systems, such as protein kinase C (PKC) (Marasco et al., 1990; Zhou and Arthur, 1997; Aroca et al., 2001; Conesa-Zamora et al., 2005).

The way these compounds are incorporated in cells is not known, although it is clear that they are finally located and carry out their functions in the cell membrane (Berdel et al., 1981a; Paltauf, 1994; Wagner et al., 2000). In this sense, a study of the interactions between these compounds and model membranes is very important since it would provide valuable information about the molecular properties that would explain their biological activity.

A compound related to these asymmetric ether phospholipids is lysophosphatidylcholine (LPC), which is produced after the hydrolysis of phosphatidylcholine by phospholipase A_2. Despite the fact that it is rapidly metabolized, it has been found to have cytotoxic effects (Burdzy et al., 1964), a finding that triggered the development of lipidic antitumor ethers, which are synthetic molecules of great metabolic stability, unlike LPC. These asymmetric ether lipids are characterized by an ether bond linking the *sn*-1 position of glycerol with a long hydrocarbon chain (Munder and Westphal, 1990).

All these compounds are structural analogs of platelet-activating factor (PAF), but lack the ester bond in the *sn*-2 position, where different groups can be found, such as a methyl group [as happens with 1-*O*-octadecyl-2-*O*-methyl-*sn*-glycero-3-phosphocholine (ET-18-*O*CH_3, or edelfosine) and 1-*O*-hexadecyl-2-*O*-methyl-*sn*-glycero-3-phosphoserine (ET-16-*O*CH_3-Ser)], an hydroxyl group [in the case of 1-*O*-octadecyl-2-*O*-hydroxy-*sn*-glycero-3-phosphocholine (ET-18-OH)], or a hydrogen atom [for example with 1-*O*-octadecyl-*sn*-glycero-3-phosphocholine (ET-18-H)]. 1-Palmitoyl-2-acetyl-*sn*-glycero-3-phosphocholine (PAPC) is another analog of PAF, which possesses a different group in the *sn*-1 position.

Only PAF and LPC occur in vivo. Fig. 1 shows the structure of these and the other compounds used in this work, all of them possessing an asymmetric structure.

It has been reported that some of these asymmetric phospholipids, such as ET-18-*O*CH_3, ET-18-OH, or PAF, can form bilayers similar to those formed by common phospholipids (Huang et al., 1986; Xie et al., 1997). Some studies have revealed that pure ether lipids can also form micelles at temperatures over the transition temperature and extended lamellar structures with interdigitated structures in the hydrocarbon chains at temperatures below the transition (Xie et al., 1997; Dick and Lawrence, 1992; Maurer et al., 1994). The interdigitated structure suggests that these molecules can easily insert themselves into the membrane, where they find their active site or produce certain membrane perturbations (Xie et al., 1996). DSC experiments have revealed that these compounds can penetrate model membranes and modify their physical properties, reducing the phase transition temperature, varying the enthalpy change, and decreasing the cooperativity in the fusion process (Noseda et al., 1988).

In this work we have used seven asymmetric phospholipids, namely ET-18-*O*CH_3, ET-16-*O*CH_3-Ser, ET-18-OH, ET-18-H, PAPC, LPC and PAF, to study their effects on the physical properties of two typical model membranes: 1,2-dimyristoyl-*sn*-glycero3-phosphocholine (DMPC) and 1,2-dielaidoyl-*sn*-glycero-3-phosphoethanolamine (DEPE). Compared with ET-18-*O*CH_3, three of these compounds (PAF, ET-18-H, and ET-18-OH) contain differences in the group of the *sn*-2 position, whereas other two (PAPC and LPC) included differences in both *sn*-1 and *sn*-2 positions. The last mentioned analog was similar to ET-18-*O*CH_3 but contained a polar head group including serine (ET-16-*O*CH_3-Ser). In order to detect the influence of these compounds on the physical properties of the model membranes, differential scanning calorimetry (DSC), ^{31}P-nuclear magnetic resonance (^{31}P NMR) spectroscopy, and X-ray diffraction studies were used.

The results indicate that asymmetric phospholipids were able to induce interdigitated membranes in DMPC below the phase transition, Additionally they inhibit the formation of the inverted hexagonal H_{II} phase in DEPE. Finally and although all these compounds have similar effects on membranes ET-18-OCH_3 had a much bigger apoptotic effect, on cultured cells, than the other six.

2. Materials and methods

2.1. Materials

1,2-Dimyristoyl-*sn*-glycero-3-phosphocholine (DMPC), 1,2-dieladoyl-*sn*-glycero-3-phosphoethanolamine (DEPE),

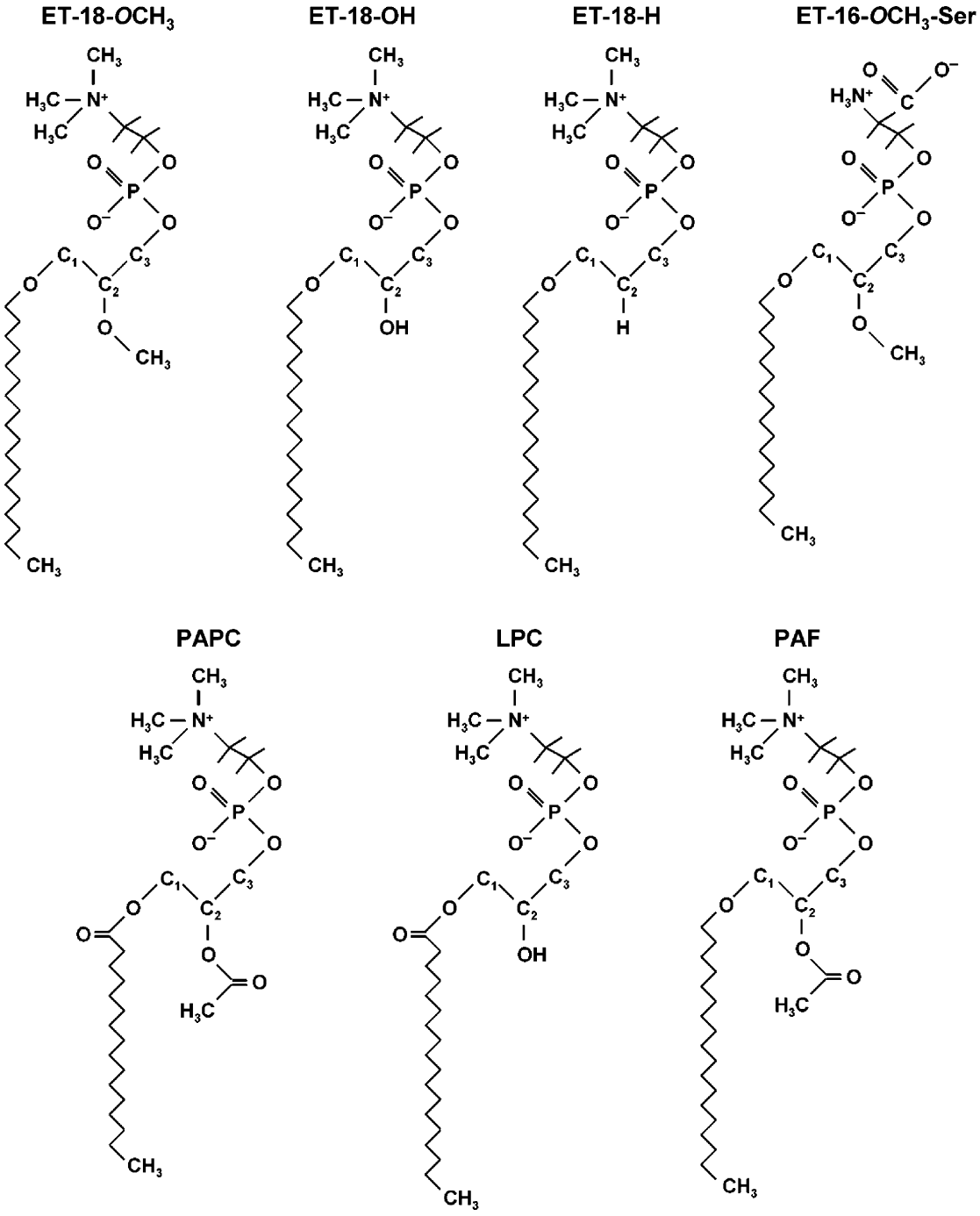

Fig. 1. Molecular schemes of the different asymmetric lipid compounds used in this work.

1-palmitoyl-2-hydroxy-*sn*-glycero-3-phosphocholine (LPC), platelet activating factor (PAF), 1-palmitoyl-2-acetyl-*sn*-glycero-3-phosphocholine (PAPC), and 1-*O*-octadecyl-2-*O*-methyl-*sn*-glycero-3-phosphocholine (ET-18-OCH_3) were purchased from Avanti Polar Lipids (Alabaster, AL, USA). 1-*O*-octadecyl-*sn*-glycero-3-phosphocholine (ET-18-H), 1-*O*-octadecyl-2-hydroxy-*sn*-glycero-3-phosphocholine (ET-18-OH), and 1-*O*-hexadecyl-2-*O*-methyl-*sn*-glycero-3-phosphocholine (ET-16-OCH_3-Ser) were obtained from INKEYSA (Barcelona, Spain) and from M. Modolell (Max-Planck-Institut für Immunbiologie, Freiburg, Germany). Water was distilled twice and deionized in a Millipore system from Millipore Ibérica (Madrid).

2.2. DSC measurements

Samples containing 3 μmol of phospholipids, DMPC, or DEPE and the appropriate amount of the different asymmetric lipids were mixed and dried under a stream of oxygen-free N_2. Then the last traces of organic solvent were removed by keeping the samples under vacuum for at least 2 h. Multilamellar vesicles were formed by incubating the dried lipids in 1.5 mL

buffer containing 20 mM Tris–HCl pH 7.5 and 100 μM EDTA, for 15 min at a temperature above the gel to fluid phase transition with occasional and vigorous vortexing. Samples were subjected to a 15-min degasifying treatment before loading into the calorimeter.

Thermograms were recorded using a Microcal MC-2 Scanning Calorimeter (Microcal, Northampton, MA, USA). The appropriate buffer was used in the reference cell. The samples were scanned over a temperature range from 7 to 50 °C (in the case of DMPC-containing samples), or from 14 to 85 °C (in the case of samples including DEPE), at a heating rate of 60 °C/h. The thermograms were analyzed with Microcal Origin 5.0 software (Microcal, Northampton, MA, USA). Baselines were created and subtracted and then the traces were normalized according to the total lipid concentration. The lipid concentration of each sample was performed analyzing the organic phosphorus included in each one, using the method described by Böttcher et al. (1961).

2.3. ^{31}P NMR spectroscopy

Samples for ^{31}P NMR were prepared by combining organic solutions containing 33.6 μmol of phospholipid (DMPC or DEPE), and the appropriate amount of the different asymmetric lipids.

Lipid mixtures were dried under a stream of oxygen-free N_2 and the last traces of organic solvent were removed by keeping the samples under vacuum for at least 2 h. Multilamellar vesicles were formed incubating the dried lipids in 1 mL buffer containing 20 mM Tris–HCl pH 7.5 and 100 μM EDTA, at 50 °C for 15 min with occasional vigorous vortexing. After this incubation, samples were centrifuged at 13,000 × *g* for 10 min and the pellets were transferred to conventional 5 mm NMR tubes.

^{31}P NMR spectra were obtained in the Fourier Transform mode in a Varian Unity 300 Spectrometer. All chemical shift values are quoted in parts per million (ppm) with reference to pure lysophosphatidylcholine micelles (0 ppm), positive values referring to low-field shifts. All spectra were obtained in the presence of a gated broad band proton decoupling (5 W input power during acquisition time), and accumulated free inductive decays were obtained from up to 5000 scans. A spectral width of 25,000 Hz, a memory of 32,000 data points, a 2 s interpulse time, and an 80° radio frequency pulse (11 μs) were used. Prior to Fourier transformation, an exponential multiplication was applied, resulting in a 60 Hz line broadening.

2.4. X-ray diffraction

Simultaneous small (SAX) and wide (WAX) angle X-ray diffraction measurements were carried out using a modified Kratky compact camera (MBraum–Graz–Optical Systems, Graz Austria), which uses two coupled linear position sensitive detectors (PSD, MBraun, Garching, Germany) to monitor the s-ranges [$s = 2\sin\theta/\lambda$, 2θ = scattering angle, $\lambda = 1.54$ Å] between 0.0075–0.07 and 0.20–0.29 $Å^{-1}$, respectively. Nickel-filtered Cu Kα X-rays were generated by a Philips PW3830 X-ray Generator operating at 50 kV and 30 mA. The position calibration of the detectors was performed by using Ag-stearate (small-angle region, *d*-spacing at 48.8 Å) and lupolen (wide-angle region, *d*-spacing at 4.12 Å) as reference materials. Samples for X-ray diffraction were prepared by mixing 15 mg of DMPC or POPC/sphyngomyelin/cholesterol (1:1:1, molar ratio) and the appropriate amount of asymmetric phospholipids in chloroform/methanol (1:1, molar ratio). Multilamellar vesicles were formed as described above for DSC measurements. After centrifugation at 13,000 × *g*, the pellets were measured in a thin-walled Mark capillary held in a steel cuvette which provides good thermal contact to the Peltier heating unit. X-ray diffraction profiles were obtained for 10 min exposure times after 10 min of temperature equilibration.

Samples for determination of structural parameters at different degree of hydration were prepared by mixing 15 mg of pure DMPC alone or in the presence of 40 mol% of LPC in chloroform/methanol (1:1, molar ratio). Samples were carefully dried and buffer was added to achieve different weight fraction of water. Samples were incubated 15 h at 30 °C, centrifuged at 13,000 rpm for 5 min, incubated 24 h at 30 °C, and then they were measured as described above.

Determination of the structural parameters at different degree of hydration were made by using the model presentation of the data described by Rand et al. (1988), which is in the form of the relation between the measured water content of the lamellar phase, the lamellar repeat spacing *d*, the thickness of the bilayer d_l, taken as a layer that contains all and only the lipid in the sample, and the distance between the bilayers d_w, equal to the thickness of a layer that contains all the water. This division of the repeat spacing follows the Luzzati tradition (Luzzati and Husson, 1962; Luzatti, 1968) of using mass average thicknesses based on measured sample composition.

Bilayer thickness, d_l, and water layer thickness or bilayer separation, d_w, are

$$d_l = \phi d \qquad d_w = (1 - \phi)d$$

where *d* is the lamellar repeat spacing and

$$\phi = \frac{1}{(1 + (1 - c)v_w)/cv_l}$$

is the volume fraction of lipid, *c* is the weight fraction of lipid in the phase, and v_w and v_l are the partial specific volumes of water and phospholipid, respectively, each taken as 1.0, according to (Cullis and de Kruijff, 1979).

2.5. Cell culture conditions

The human acute myeloid leukemia HL-60 cell line was grown in RPMI 1640 supplemented with 10% (v/v) heat-inactivated fetal calf serum, 2 mM L-glutamine, 100 units/mL penicillin, and 24 μg/mL gentamicin. Cells were incubated at 37 °C in a humidified atmosphere of 5% CO_2 and 95% air.

2.6. Apoptotic assays

The induction of apoptosis was monitored as the appearance of the sub-G_l peak in cell cycle analysis (Gajate et al., 2000).

Briefly, cells (5×10^5) were centrifuged and fixed overnight in 70% ethanol at 4 °C. Cells were washed three times with PBS, incubated for 1 h with 1 mg/mL Rnase A and 20 μg/mL propidium iodide at room temperature, and then analyzed for cell cycle with a Becton Dickinson FACSCalibur flow cytometer (San Jose, CA). Quantitation of apoptotic cells was calculated as the percentage of cells in the sub-G_1 region (hypodiploidy) in cell cycle analysis.

3. Results and discussion

3.1. Thermal study of the DMPC mixtures

DSC was used to determine the effect of increasing concentrations of the different asymmetric phospholipids on the phase transition of pure DMPC. The pure DMPC thermogram showed a pre-transition, with a T_c at 13 °C, and a very cooperative main transition, beginning at 23.5 °C (Fig. 2). The presence of increasing concentrations of the different asymmetric phospholipids led to several changes in the thermograms obtained.

In the case of ET-18-*O*CH_3 (Fig. 2A), a relatively low proportion of this ether (5 mol%) affected both the pre-transition and the main transition, which appeared at lower temperatures. The first became more diffuse and started at about 9 °C, while the second started at 22.8 °C. Similar effects were detected with 10 mol% of the asymmetric lipid, with the main transition starting at lower temperature, i.e. 21.6 °C. In the presence of 25 mol% ET-18-*O*CH_3, the pre-transition disappeared and the main transition, which started at 22.3 °C, showed a shoulder toward higher temperatures, probably indicating the presence of two components. With 40 mol% ET-18-*O*CH_3, the main transition became narrower, with just one component, and the transition temperature (T_c) occurred at 24.9 °C. The T_c with 50 mol% ET-18-*O*CH_3 was at 25.3 °C. Higher concentrations of ET-18-*O*CH_3 produced a decrease in the cooperativity, with broader transitions. The same trend was shown with 60 mol% ET-18-*O*CH_3, the transition becoming broader and beginning at 24.8 °C, while in the presence of 70 mol% ET-18-*O*CH_3, the area under the transition peak decreased, probably indicating the solubilization of a significant proportion of DMPC molecules, which no longer participated in the transition, while T_c appeared at 21.6 °C. No transition was detected in the sample containing 80 mol% ET-18-*O*CH_3 so that solubilization was total at this percentage.

Similar results were observed when LPC was used, although the pre-transition was not present with 10 mol%. Moreover, the second component appeared pure at 50 mol% and total solubilization was reached at 70 mol% (Fig. 2B).

Qualitatively similar results were also observed for other analogs (not shown for the sake of brevity). In the case of ET-18-OH, the pre-transition was not present above 25 mol%, whereas the pure second component was detected at 50 mol%, and total solubilization was not observed even at 90 mol%; ET-18-H behaved exactly as ET-18-OH; in PAPC the pre-transition was not observed above 25 mol%, the pure second component was detected at 40 mol% and total solubilization appeared above 70 mol%; and with PAF the pre-transition was not detected above 25 mol%, the pure second component appeared at 40 mol% and total solubilization was observed at 80 mol%.

The effect of ET-16-*O*CH_3-Ser, however, was different (Fig. 2C). The pre-transition had already disappeared at 10 mol%, and the main transition shifted towards a lower temperature, starting in this case at 22 °C. Moreover, this transition was asymmetric and showed a small shoulder at high temperature, but finished at 26.5 °C. With 25 mol%, the transition became

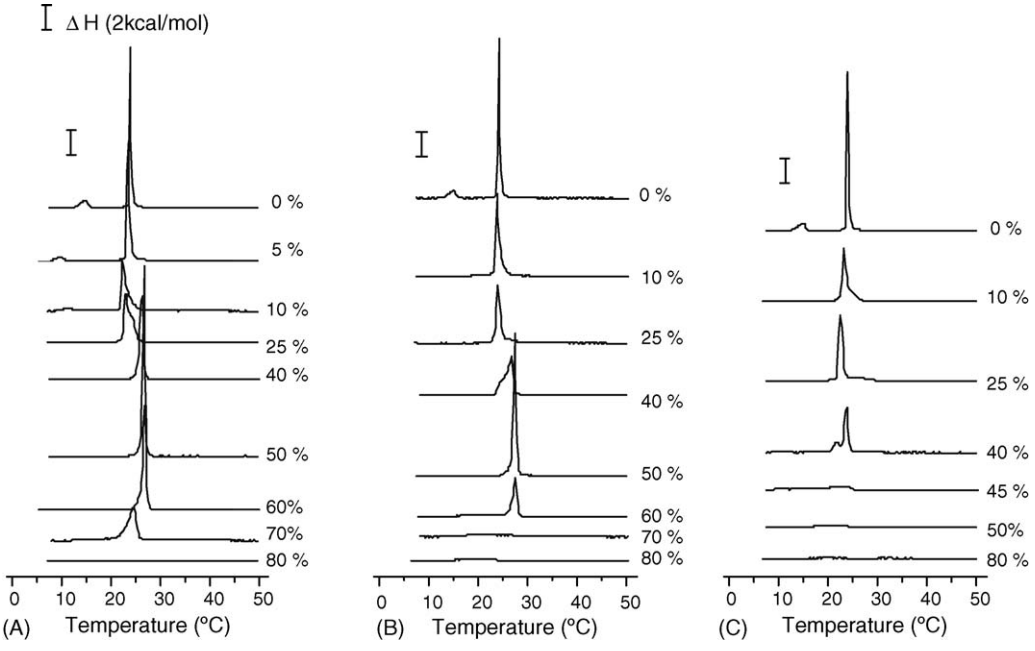

Fig. 2. DSC heating thermograms of aqueous dispersions of mixtures of DMPC with different proportions of ET-18-*O*CH_3 (A), LPC (B), and ET-16-*O*CH_3-Ser (C). The heating rate was 60 °C/h. The mol% of the different asymmetric lipids in the mixtures is indicated on the right hand side of each thermogram.

broader and diffuse, extending from 21.6 to 29.1 °C, with the main peak centered at 22 °C. The addition of 40 mol% produced a broad transition, from 20.4 to 24.6 °C, which was composed of two partially overlapping peaks. The first was smaller and centered at 21.5 °C, while the second was located at 23.5 °C. With 45 mol% ET-16-*O*CH_3-Ser, the transition was very broad, from 15.6 to 25.1 °C, and the two components remained, with the first peak appearing at 17.5 °C. The sample including 50 mol% again showed a very broad and diffuse transition, which extended from 10 to 28.9 °C. This transition almost disappeared with 80 mol% ET-16-*O*CH_3-Ser, indicating total solubilization.

3.2. ^{31}P NMR spectroscopy of the DMPC mixtures

^{31}P NMR spectroscopy was used to obtain additional information about the organization of the lipid mixtures below (at 15 °C) and above (at 35 °C) the main phase transition observed by DSC. Pure DMPC showed asymmetric spectra both below and above the phase transition (Fig. 3A), with a high-field peak and a low-field shoulder, characteristic of an axially symmetrical shift tensor and consistent with the arrangement of the phospholipids in a bilayer configuration. The lineshapes were broad with a chemical shift anisotropy ($\Delta\sigma$) of 62 ppm at 15 °C,

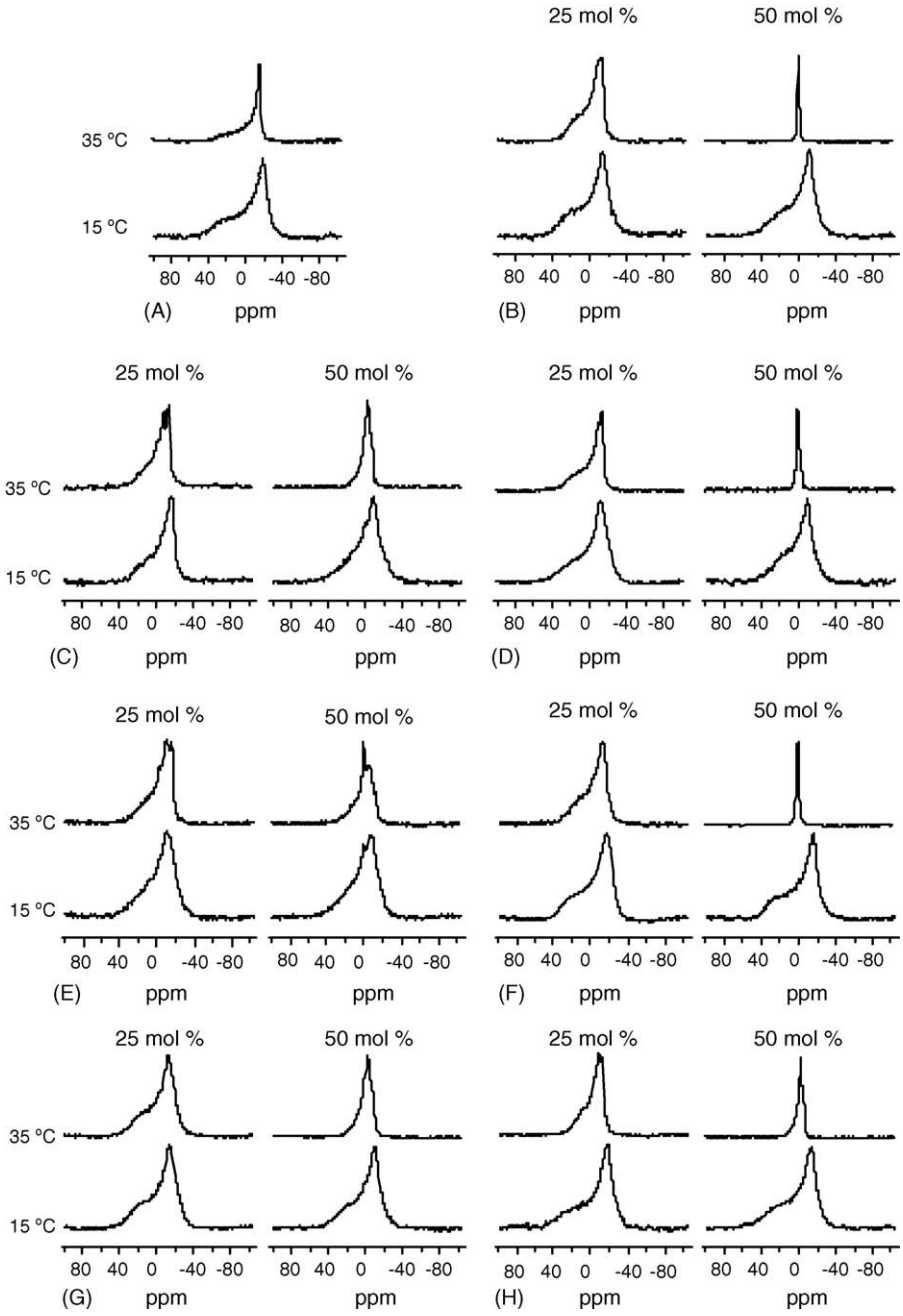

Fig. 3. ^{31}P NMR spectra of aqueous dispersions of mixtures of pure DMPC (A), and DMPC with different proportions of ET-18-*O*CH_3 (B), ET-18-OH (C), ET-18-H (D), ET-16-*O*CH_3-Ser (E), PAPC (F), LPC (G), and PAF (H). Each sample was measured at two different temperatures, below (15 °C) and above (35 °C) the transition temperature, as shown on the left. The concentrations of the asymmetric lipids were 25 or 50 mol%, as indicated on top of each spectrum.

and 46 ppm at 35 °C. According to the DSC results commented above, the sample is in gel state at 15 °C and in fluid state at 35 °C.

The addition of 25 mol% ET-18-*O*CH_3 produced similar spectra to those seen at the same temperatures of the pure phospholipid, with a $\Delta\sigma$ of 58 ppm at 15 °C and 40 ppm at 35 °C (Fig. 3B). In the presence of 50 mol% ET-18-*O*CH_3, a similar lineshape was obtained at 15 °C, with a $\Delta\sigma$ of 51 ppm, while at 35 °C, the lineshape showed an isotropic signal with a $\Delta\sigma$ of 2.1 ppm (Fig. 3B). This type of signal has been related previously to small vesicles or a micelle and small vesicle mixture (Cullis and de Kruijff, 1979).

The addition of 25 mol% ET-18-OH produced a lineshape characteristic of a bilayer configuration with a $\Delta\sigma$ of 50 ppm at 15 °C and 32 ppm at 35 °C (Fig. 3C). It is of note that at 15 °C the intensity of the low-field peak increased, probably pointing to smaller vesicles (Traikia et al., 2000; Burnell et al., 1980), and that at 35 °C another broad isotropic peak was detected, also corresponding probably to small vesicles. In the presence of 50 mol% ET-18-OH (Fig. 3C), the lineshape at 15 °C was asymmetric and corresponded to a bilayer configuration with a $\Delta\sigma$ of about 49 ppm, although an isotropic component was already evident. The lineshape at 35 °C was mainly isotropic, corresponding to small vesicles and/or micelles. Nevertheless, the bilayer configuration was still present at this temperature, as could be seen from the small low-field peak.

The presence of 25 mol% ET-18-H gave rise to asymmetric lineshapes at both 15 ($\Delta\sigma$ of 68 ppm) and 35 °C ($\Delta\sigma$ of 42 ppm), with a small peak denoting an isotropic phase at 35 °C (Fig. 3D). With 50 mol% ET-18-H, the lineshape at 15 °C was still asymmetric ($\Delta\sigma$ of 50 ppm), but the low-field peak was greater, pointing to a decrease in vesicle size. At 35 °C, an isotropic peak was observed with a $\Delta\sigma$ of 4.8 ppm, although a small low-field peak was still detected, suggesting the presence of vesicles in bilayer configuration.

The addition of 25 mol% ET-16-*O*CH_3-Ser produced lineshapes which were different from those obtained for the pure DMPC, although they were asymmetric and consistent with a bilayer configuration (Fig. 3E). The $\Delta\sigma$ was 52 ppm at 15 °C and 38 ppm at 35 °C, at which temperature, another two peaks were detected, probably corresponding to the separation of the ether phosphorus bound to serine from the phospholipid phosphorus bound to choline. In fact, at 15 °C the signal from ether phosphorus can be slightly detected. The addition of 50 mol% ET-16-*O*CH_3-Ser (Fig. 3E) produced an asymmetric lineshape at 15 °C, with a $\Delta\sigma$ of 54 ppm, and a small isotropic peak at 0 ppm. At 35 °C, this isotropic signal increased, although the bilayer component was preserved. The $\Delta\sigma$ was 34 ppm. With both 25 and 50 mol%, and especially in the fluid state, there was an increase in the intensity of the low-field peak, corresponding probably to a decrease in the vesicle size.

The lineshapes including 25 mol% PAPC (Fig. 3F) were very similar to those obtained with the pure DMPC at both temperatures, i.e. a bilayer configuration with a $\Delta\sigma$ of 57 ppm at 15 °C and 42 ppm at 35 °C. The addition of 50 mol% PAPC (Fig. 3F) produced an asymmetric lineshape at 15 °C with a $\Delta\sigma$ of 58 ppm and a small isotropic component. At 35 °C, the lineshape was mainly isotropic with a $\Delta\sigma$ of 4 ppm, probably corresponding to small vesicles.

The addition of 25 mol% LPC produced asymmetric lineshapes, with a $\Delta\sigma$ of 57 ppm at 15 °C and 46 ppm at 35 °C (Fig. 3G). At both temperatures, a small isotropic component was detected. In the presence of 50 mol% LPC (Fig. 3G), the asymmetric lineshape at 15 °C ($\Delta\sigma$ of 51 ppm) showed a small isotropic component, whereas at 35 °C the broad isotropic peak centered at 0 ppm overlapped a small bilayer configuration signal ($\Delta\sigma$ of 24 ppm).

Finally, the addition of 25 mol% PAF (Fig. 3H) produced asymmetric lineshapes at 15 °C ($\Delta\sigma$ of 64 ppm) and 35 °C ($\Delta\sigma$ of 32 ppm). At 35 °C, an isotropic signal was also detected, whereas the low-field peak was higher than in the case of pure DMPC, suggesting the presence of smaller vesicles. In the presence of 50 mol% PAF (Fig. 3H), the lineshape at 15 °C was asymmetric, with a $\Delta\sigma$ of 58 ppm, while at 35 °C an isotropic peak was observed overlapping a small signal denoting bilayer organization ($\Delta\sigma$ of 16 ppm). This lineshape suggests that the vesicle size is even smaller than in the sample including 25 mol% PAF.

An apparent disagreement between the DSC and the ^{31}P NMR spectroscopy data appeared in the case of the sample including 50 mol% ET-18-OCH_3. There was an extremely cooperative phase transition, as seen by DSC, but the ^{31}P NMR spectroscopy lineshape showed only one narrow isotropic peak at a Ds of 2.1 ppm. This fact could result from the high degree of cooperativity in the interdigitated complex, although with small vesicles, yielding isotropic spectra. This would be the case, if interdigitated structures were adopted, such as those described in previous papers with similar asymmetric ether lipids (Olivier et al., 1991). Similar problems were detected with 50 mol% PAPC, PAF, or LPC.

3.3. X-ray diffraction of DMPC mixtures

Information on the structural characteristics of DMPC/asymmetric lipid systems was obtained by X-ray diffraction measurements. Small-angle X-ray diffraction was used to check whether asymmetric lipids affected the phase behavior of DMPC. This technique not only defines the macroscopic structure itself, but also provides the interlamellar repeat distance in the lamellar phase. The first order reflection component corresponds to the interlamellar repeat distance, which is comprised of the bilayer thickness and the thickness of the water layer between bilayers. Fig. 4 shows the SAXS diffraction pattern profiles corresponding to pure DMPC and DMPC containing asymmetric phospholipids at two different temperatures, below and above the phase transition, i.e. at 12 °C (Fig. 4A) and 35 °C (Fig. 4B). The pure DMPC system exhibited diffraction profiles with sharp Bragg reflections and with distances related as 1:1/2:1/3, which are characteristic of the expected multilamellar organization (Luzatti, 1968). Pure DMPC diffraction profiles also showed lamellar repeat distances of 64 Å in the gel phase (at 12 °C, Fig. 4A) and 61 Å in the liquid crystalline phase (at 35 °C, Fig. 4B).

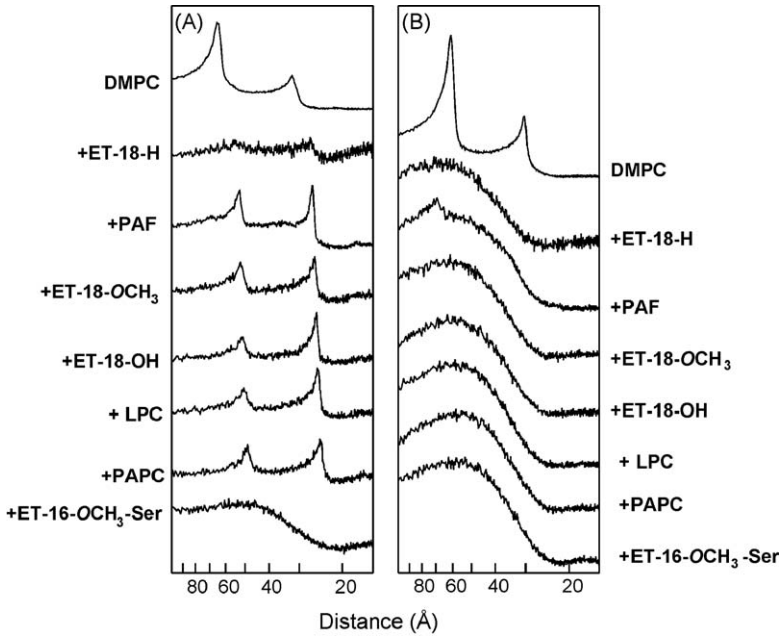

Fig. 4. Small-angle X-ray diffraction profiles at 12 °C (A) and 35 °C (B), obtained from (top to bottom) pure DMPC, DMPC containing 40 mol% ET-18-H, PAF, ET-18-*O*CH_3, ET-18-OH, LPC, PAPC and ET-16-*O*CH_3-Ser.

At 12 °C (Fig. 4A), the different DMPC/asymmetric phospholipid systems (3:2, molar ratio) always showed reflections which related as 1:1/2:1/3, indicating that the system remained in the lamellar state. However, the interlamellar repeat distances observed in the presence of asymmetric lipids were drastically decreased when compared with the pure DMPC, and were found in the range of 49–54 Å. In the case of ET-16-*O*CH_3-Ser, instead of sharp Bragg reflections, the diffraction profile exhibited a broad scattering band centered at 49 Å. The reflections characteristic of pure DMPC in the liquid crystalline phase (35 °C, Fig. 4B) were replaced in the presence of asymmetric phospholipids by broad scattering bands.

The interlamellar repeat distance reflects the thickness of the bilayer, so a decrease in the interlamellar repeat distance indicates a decrease in the thickness of the lipid bilayer. One of the important characteristics of interdigitated bilayers is the decreased thickness of the lipid bilayer, because of the insertion of acyl chains into the opposite layer of the bilayer. The findings that asymmetric lipids reduce the interlamellar repeat distance of DMPC by 10–15 Å is a direct evidence that these compounds induce DMPC bilayers to perform the transition from gel to the interdigitated gel phase. In the presence of asymmetric lipids we obtained a wide-angle diffractogram with one sharp and symmetric peak at 4.1 Å, which is similar to that reported for the interdigitated gel phase of DMPC in the presence of ethanol (Winter et al., 2001), which supports our conclusion for untilted, and therefore interdigitated hydrocarbon chains in order to account for the small interlamellar repeat distance. All these results reveal that the main effect of asymmetric lipids on DMPC bilayers is to induce an interdigitated structure in the gel phase.

Previous studies have shown that some asymmetric phospholipids may form interdigitated structures when used alone, as is the case for ET-18-*O*CH_3 (Maurer et al., 1994; Xie et al., 1996), PAF (Huang et al., 1986; Xie et al., 1996) and lyso-PAF (Xie et al., 1996). Some of these asymmetric phospholipids like PAF,

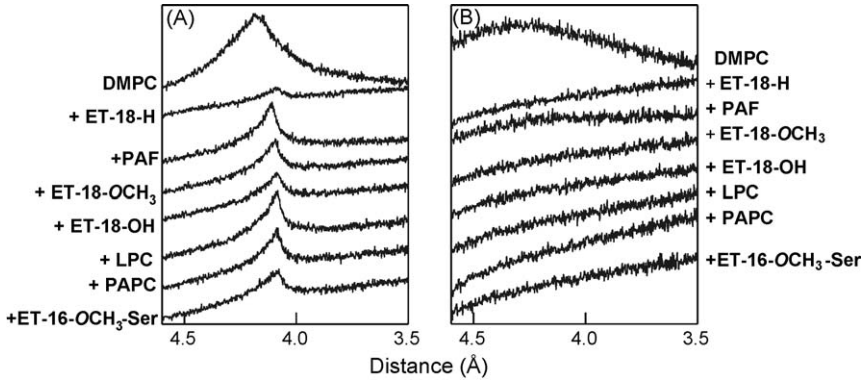

Fig. 5. Wide-angle X-ray diffraction profiles at 12 °C (A) and 35 °C (B), obtained from (top to bottom) pure DMPC, DMPC containing 40 mol% ET-18-H, PAF, ET-18-*O*CH_3, ET-18-OH, LPC, PAPC and ET-16-*O*CH_3-Ser.

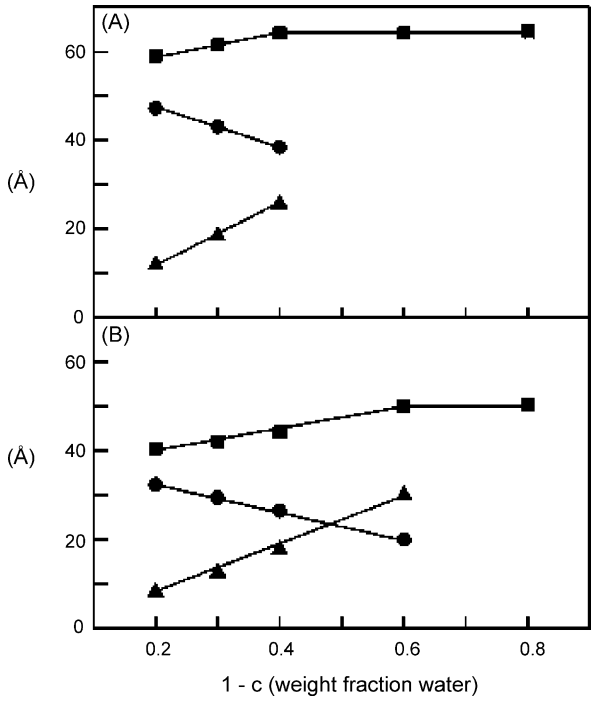

Fig. 6. Structural parameters of the lamellar phase formed at 10 °C by pure DMPC (A) and DMPC containing 40% of LPC (B) as they vary with water content. Lamellar repeat spacing, d (■); thickness of the bilayer, d_l (●), and bilayer separation, d_w (▲).

lysoPAF and LPC have also been described as inducing interdigitated phases in DMPC (Olivier et al., 1991). The wide-angle X-ray diffraction patterns of pure DMPC and DMPC/asymmetric phospholipids systems at the same temperatures are shown in Fig. 5. At 12 °C (Fig. 5A), pure DMPC showed a broad asymmetric peak centered at 4.18 Å, which is typical for lipid bilayers in the lamellar gel phase with tilted hydrocarbon chains and pseudohexagonal chain packing (Tardieu et al., 1973). In the DMPC/asymmetric lipids systems (3:2, molar ratio) a single sharp reflection appeared at around 4.1 Å, which indicates that the hydrocarbon chains were packed in a hexagonal lattice and the direction of acyl chains was perpendicular to the membrane surface (Adachi et al., 1995). Above the main transition temperature (35 °C, Fig. 5B), pure DMPC showed a very broad component centered at 4.35 Å, typical for unordered lipid chains in the liquid crystalline phase. In the presence of asymmetric phospholipids, a diffuse reflection was always recorded above the main phase transition.

To discard the possibility that the observed reduction in the lamellar repeat spacing in the small-angle diffractograms could reflect a reduction in the hydration of the samples containing ether lipids and not an effective reduction of the bilayer thickness, we studied the structural dimensions of the lamellar phase formed by pure DMPC and DMPC containing 40% LPC, in defined amounts of water and at 12 °C. Fig. 6 shows the dependence of the lamellar repeat spacing, d, and bilayer (d_l) and water (d_w) thicknesses as they vary with water content. It is clearly shown that for any water content studied, the interbilayer distance (d_l) for the sample containing LPC is always 15–20 Å shorter than that of the pure phospholipid. LPC sample at low hydration (20–40% water) shows an additional bilayer signal which was shorter than that of pure DMPC and which was not present at higher hydration (not shown). Maximum hydration of the lipid can be determined from the relation between the lamellar repeat spacing (d) and the weight fraction of lipid in the phase (Rand et al., 1988). The maximum amount of water uptake can be estimated from the intersection of the horizontal line representing the average repeat spacing in excess water with the line that relates d and c in the region of restricted water. The lamellar repeat spacing presented in Fig. 6 shows that while pure DMPC can uptake about 40% of water, the presence of LPC produced an increase in the hydration which reaches 60% water.

3.4. Thermal study of the DEPE mixtures

DSC was used to determine the effect of increasing concentrations of the different asymmetric phospholipids on the phase transition of pure DEPE. The pure DEPE thermogram showed a very cooperative main transition at 38.5 °C (from 37.1 to 38.9 °C) and a small transition at 66.5 °C (from 65.1 to 66.5 °C) (Fig. 7). The first showed the transition from lamellar gel phase (L_β) to lamellar liquid crystalline phase (L_α), whereas the second reflected the transition from lamellar liquid crystalline phase (L_α) to inverted hexagonal phase (H_{II}).

The addition of ET-18-OCH$_3$ affected both transitions (Fig. 7). The cooperativity of the main transition decreased with

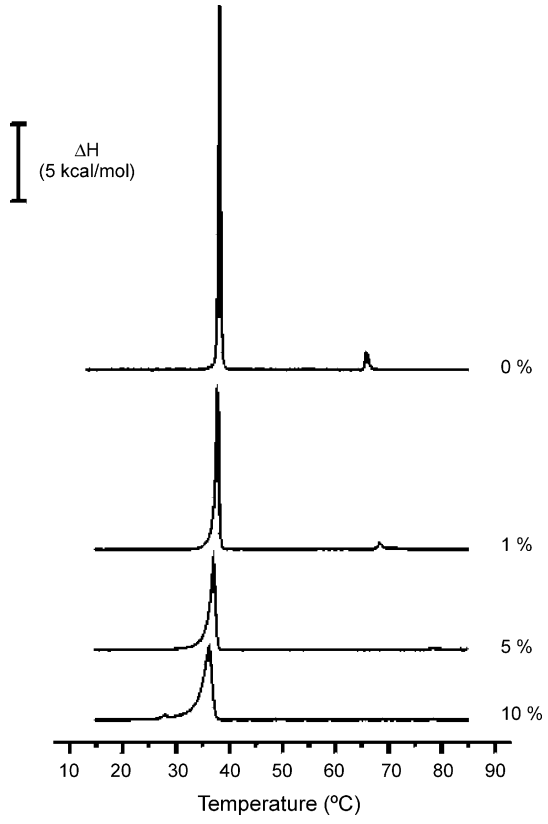

Fig. 7. DSC heating thermograms of aqueous dispersions of mixtures of DEPE with different proportions of ET-18-OCH$_3$. The heating rate was 60 °C/h. The mol% of the asymmetric lipid in the mixtures is indicated on the right hand side of each thermogram.

increasing concentrations of this ether lipid, i.e. the enthalpy change was reduced, and moved to lower temperatures: 37.5 °C with 1 mol%, and 36.7 °C with 5 mol%. Furthermore, with 10 mol% ET-18-*O*CH_3, the main transition was located at 36 °C and a new small peak appeared preceding it, at 25.5 °C, as observed in previous studies (Sánchez-Piñera et al., 1999; Salgado et al., 1993). The transition from L_α to H_{II} phase was also affected by ET-18-*O*CH_3. Firstly, the transition moved to higher temperatures, starting at 67.3 °C with 1 mol% ET-18-*O*CH_3, and at 76.9 °C with 5 mol%. At this latter concentration, the L_α to H_{II} phase transition was hardly detected and finally disappeared with 10 mol%.

The effects of ET-18-OH, ET-18-H, ET-16-*O*CH_3-Ser, PAPC, LPC and PAF on DEPE vesicles were very similar to those produced by ET-18-*O*CH_3 and are not shown for the sake of brevity.

3.5. ^{31}P NMR spectroscopy of the DEPE mixtures

In order to complete the information about the physical organization of DEPE vesicles containing these asymmetric lipids, ^{31}P NMR spectroscopy was used (Fig. 8). Samples were prepared by including 5 mol% of each asymmetric lipid, because, in most cases, the transition from L_α to H_{II} phase could still be detected at this concentration. Three different temperatures were selected for this study: 25 °C (in the lamellar gel phase, L_β), 50 °C (in the lamellar liquid crystalline phase, L_α) and 85 °C (in the inverted hexagonal phase, H_{II}).

The pure DEPE lineshape was asymmetric (Fig. 8A), showing a high-field peak and a low-field shoulder at 25 °C, characteristic of phospholipids in bilayer configuration. The $\Delta\sigma$ was 64 ppm, suggesting the gel state. At 50 °C, bilayer configuration was still detected, but the $\Delta\sigma$ was 42 ppm, indicating a fluid state. Finally, at 85 °C, the lineshape showed a low-field peak and a high-field shoulder, which is characteristic of an inverted H_{II} hexagonal phase.

When 5 mol% ET-18-*O*CH_3 was included (Fig. 8B), a similar spectrum to that of pure DEPE was recorded at 25 °C, with a $\Delta\sigma$ of 60 ppm. At 50 °C, a small isotropic component centered at 0 ppm was detected overlapping a peak typical of a bilayer configuration in fluid state ($\Delta\sigma$ of 44 ppm). At 85 °C, the bilayer configuration in fluid state ($\Delta\sigma$ of 34 ppm) was still present, and a small isotropic component was also detected.

The sample including 5 mol% ET-18-OH (Fig. 8C) showed a spectrum at 25 °C with a lineshape characteristic of bilayer configuration (a high-field peak and a low-field shoulder) in gel

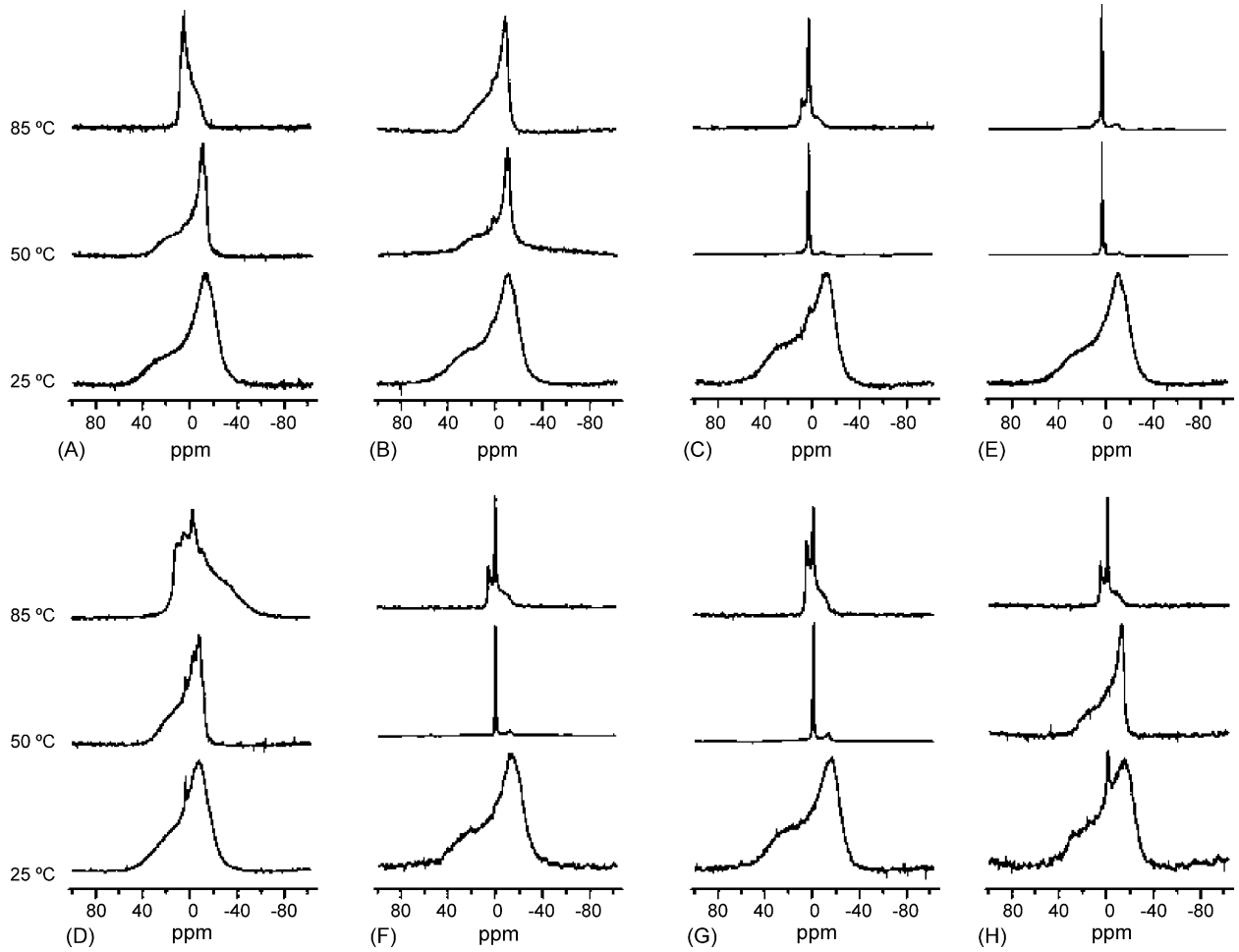

Fig. 8. ^{31}P NMR spectra of aqueous dispersions of mixtures of pure DEPE (A), and DEPE with 5 mol% ET-18-*O*CH_3 (B), ET-18-OH (C), ET-18-H (D), ET-16-*O*CH_3-Ser (E), PAPC (F), LPC (G), and PAF (H). Samples were recorded at three different temperatures, as indicated on the left.

state ($\Delta\sigma$ of 64 ppm), with a small isotropic signal. At 50 °C, the spectrum changed completely, showing an isotropic peak with a $\Delta\sigma$ of 1.8 ppm, characteristic of small vesicles and/or micelles (Heimburg et al., 1991; Salgado et al., 1993; López-Garcia et al., 1994; Grau et al., 2000), and a very small high-field peak, which was probably due to part of the phospholipids adopting a bilayer configuration. At 85 °C, an isotropic peak overlapping the typical H_{II} inverted hexagonal phase lineshape was detected.

Similar results to those of ET-18-OH were observed with 5 mol% ET-18-H (Fig. 8D). The only difference was detected at 85 °C, where the isotropic peak was the main signal although it was overlapped by both rather small bilayer and inverted hexagonal phase configuration signals, as seen from the small peaks located at high- and low-field, respectively. This result suggests that vesicles with bilayer configuration are probably present but are not included in the hexagonal tubules.

The sample with 5 mol% ET-16-*O*CH_3-Ser at 25 °C (Fig. 8E) showed a spectrum with a lineshape characteristic of a bilayer configuration in gel state ($\Delta\sigma$ of 53 ppm), and a small isotropic signal. The same was true at 50 °C, but in a fluid state ($\Delta\sigma$ of 40 ppm) and with another bilayer configuration signal probably arising from the ether lipid phosphorus. At 85 °C, several signals from H_{II} inverted hexagonal, isotropic and bilayer structures overlapped.

When 5 mol% PAPC was added (Fig. 8F), the spectrum at 25 °C showed a bilayer configuration in gel state ($\Delta\sigma$ of 63 ppm). The low-field shoulder presented higher intensity, suggesting the presence of larger vesicles, as mentioned above. At 50 °C, an isotropic peak with a $\Delta\sigma$ of 1.8 ppm was detected with a small bilayer configuration signal, whereas at 85 °C the same isotropic peak was overlapped by both bilayer and inverted hexagonal components.

Very similar results to those mentioned for PAPC were detected with 5 mol% LPC (Fig. 8G). The only differences were that the isotropic peak was a little broader ($\Delta\sigma$ of 2 ppm), and the H_{II} inverted hexagonal component was more important at 85 °C.

Finally, the sample including 5 mol% PAF (Fig. 8H) showed a spectrum at 25 °C with a lineshape characteristic of a bilayer configuration in gel state ($\Delta\sigma$ of 58 ppm), and a quite broad isotropic peak centered at 0 ppm. A similar spectrum was recorded at 50 °C, with two differences: the lineshape had become wider ($\Delta\sigma$ of 42 ppm), indicating a fluid state, and the isotropic peak at 0 ppm was reduced. At 85 °C the spectrum indicated the presence of an H_{II} inverted hexagonal state, overlapping an isotropic signal.

All seven asymmetric lipids affected the L_α to H_{II} phase transition of DEPE, inhibiting the formation of inverted hexagonal phases in the case of ET-18-*O*CH_3, or reducing this formation in the case of the rest of asymmetric lipids. In the case of ET-18-*O*CH_3, only small isotropic signals were detected at both 50 and 85 °C, with a predominance of bilayer configuration at the higher temperature. This effects was in perfect agreement with the previous DSC data discussed above, where no signal of L_α to H_{II} inverted hexagonal phase transition was detected in the thermogram.

Table 1
Effect of ET-18-*O*CH_3 and several structurally related compounds on the induction of apoptosis in human leukemic HL-60 cells

Chemical structure	Apoptosis (%)
Control (untreated cells)	2.5 ± 0.8
ET-18-*O*CH_3	71.8 ± 3.6
ET-18-OH	2.9 ± 0.9
ET-18-H	2.9 ± 1.1
ET-16-*O*CH_3-Ser	4.2 ± 2.1
PAPC	2.8 ± 0.8
PAF	4.1 ± 0.9
LPC	3.2 ± 1.0

Cells were treated with the compounds listed below (10 μM) for 24 h in culture medium containing 10% heat-inactivated FCS, and apoptosis was then quantitated as percentage of cells in the sub-G_1 region (hypodiploidy) in cell cycle analysis by flow cytometry as described in Section 2. Data are shown as mean values ± S.D. from three different experiments.

3.6. Cell apoptosis assays

The effect of ET-18-OCH_3 and the other structurally related compounds on the induction of apoptosis in human leukemic HL-60 cells is shown in Table 1. It can be seen that ET-18-OCH_3 induced a potent apoptotic response (71.8% apoptosis), whereas the other compounds failed to promote cell death.

3.7. Biological implications

Lipids promoting non-lamellar phases, such as H_{II} hexagonal inverted phase, have been related with several biological processes (Seddon, 1990; Epand, 1990). The fact that these asymmetric lipids inhibit the tendency of DEPE to adopt inverted hexagonal phase gives them a putative key role in the signaling pathways because they can inhibit important enzymes such as PKC (Epand, 1990) or phospholipases (Zidovetzki, 1997). It has been shown in fact that ET-18-*O*CH_3, at certain concentrations, inhibit PKC enzymes (Aroca et al., 2001; Conesa-Zamora et al., 2005).

It is remarkable that the seven asymmetric phospholipids used have similar effects on DMPC membranes and a similar capacity to inhibit the tendency of DEPE to form hexagonal phases. However it is shown that, of the seven asymmetric lipids studied here, only ET-18-*O*CH_3 is capable of inducing apoptosis in cancer cells, so that other factors may be implicated, such as for example the presence of specific proteins. This notion is supported by recent work showing that Fas proteins may be involved in the action of ET-18-*O*CH_3 (Gajate and Mollinedo, 2001; Gajate et al., 2004). More work is needed to clarify this.

In addition, it is interesting that asymmetric phospholipids are able to induce interdigitated structures in DMPC vesicles below the phase transition and small vesicles and/or micelles at temperatures above the phase transition, and these properties should be taken into account when designing liposome pharmaceutical formulations of ET-18-*O*CH_3 and similar lipids.

Acknowledgements

This paper was supported by Grant 1FD97-0622 from the European Commission and Comisión Interministerial de Ciencia y Tecnología, Grant BFU2005-02482/BMC (to J.C.G.F.) from Dirección General de Investigación (Spain), Grant 00591/PI/04 (to J.C.G.F.) from Fundación Séneca (Comunidad Autónoma de Murcia, Spain), and Grant FIS04-0843 from Fondo de Investigación Sanitaria (to F.M.). C.G. and S.C.-G were supported by the Ramón y Cajal Program from the Ministerio de Educación y Ciencia of Spain.

References

Adachi, T., Takahashi, H., Ohki, K., Hatta, I., 1995. Interdigitated structure of phospholipid-alcohol systems studied by x-ray diffraction. Biophys. J. 68, 1850–1855.

Aroca, J.D., Sánchez-Piñera, P., Corbalán-García, S., Conesa-Zamora, P., de Godos, A., Gómez-Fernández, J.C., 2001. Correlation between the effect of the anti-neoplastic ether lipid 1-*O*-octadecyl-2-*O*-methyl-glycero-3-phosphocholine on the membrane and the activity of protein kinase C alpha. Eur. J. Biochem. 268, 6369–6378.

Berdel, W.E., Bausert, W.R., Fink, U., Rastetter, J., Munder, P.G., 1981a. Anti-tumor action of alkyl-lysophospholipids. Anticancer Res. 1, 345–352.

Berdel, W.E., Fink, U., Egger, B., Reichert, A., Munder, P.G., Rastetter, J., 1981b. Inhibition by alkyl-lysophospholipids of tritiated thymidine uptake in cells of human malignant urologic tumors. J. Natl. Cancer Inst. 66, 813–817.

Berdel, W.E., Fromm, M., Fink, U., Pahlke, W., Bicker, U., Reichert, A., Rastetter, J., 1983. Cytotoxicity of thioether-lysophospholipids in leukemias and tumors of human origin. Cancer Res. 43, 5538–5543.

Berdel, W.E., Greiner, E., Fink, U., Zanker, K.S., Stavrou, D., Trappe, A., Fahlbusch, R., Reichert, A., Rastetter, J., 1984. Cytotoxic effects of alkyl-lysophospholipids in human brain tumor cells. Oncology 41, 140–145.

Besson, P., Gore, J., Vincent, E., Hoinard, C., Bougnoux, P., 1996. Inhibition of Na^+/H^+ exchanger activity by an alkyl-lysophospholipid analogue in a human breast cancer cell line. Biochem. Pharmacol. 51, 1153–1158.

Böttcher, C.J.F., Van Gent, C.M., Pries, C., 1961. A rapid and sensitive submicro phosphorus determination. Anal. Chim. Acta 24, 203–204.

Brachwitz, H., Vollgraf, C., 1995. Analogs of alkyllysophospholipids: chemistry, effects on the molecular level and their consequences for normal and malignant cells. Pharmacol. Ther. 66, 39–82.

Burdzy, K., Munder, P.G., Fisher, H.Z., Westphal, O., 1964. Increase in the phagocytosis of peritoneal macrophages by lysolecithin. Z. Naturforsch. B 19, 1118–1120.

Burnell, E.E., Cullis, P.R., de Kruijff, B., 1980. Effects of tumbling and lateral diffusion on phosphatidylcholine model membrane ^{31}P NMR lineshapes. Biochim. Biophys. Acta 603, 63–69.

Conesa-Zamora, P., Mollinedo, F., Corbalán-García, S., Gomez-Fernandez, J.C., 2005. A comparative study of the effect of the antineoplasic ether lipid 1-*O*-octadecyl-2-*O*-methyl-glycero-3-phosphocholine and some homologous compounds on PKCα and PKCε. Biochim. Biophys. Acta 1687, 110–119.

Cullis, P.R., de Kruijff, B., 1979. Lipid polymorphism and the functional roles of lipids in biological membranes. Biochim. Biophys. Acta 559, 399–420.

Denizot, Y., Desplat, V., Drouet, M., Bertin, F., Melloni, B., 2001. Is there a role of platelet-activating factor in human lung cancer? Lung Cancer 33, 195–202.

Dick, D.L., Lawrence, D.S., 1992. Physicochemical behavior of cytotoxic ether lipids. Biochemistry 31, 8252–8257.

Epand, R.M., 1990. Relationship of phospholipid hexagonal phases to biological phenomena. Biochem. Cell Biol. 68, 17–23.

Gajate, C., Mollinedo, F., 2001. The antitumor ether lipid ET-18-OCH(3) induces apoptosis through translocation and capping of Fas/CD95 into membrane rafts in human leukemic cells. Blood 98, 3860–3863.

Gajate, C., Mollinedo, F., 2002. Biological activities, mechanisms of action and biomedical prospect of the antitumor ether phospholipid ET-18-OCH(3) (edelfosine), a proapoptotic agent in tumor cells. Curr. Drug Metab. 3, 491–525.

Gajate, C., Del Canto-Janez, E., Acuna, A.U., Amat-Guerri, F., Geijo, E., Santos-Beneit, A.M., Veldman, R.J., Mollinedo, F., 2004. Intracellular triggering of Fas aggregation and recruitment of apoptotic molecules into Fas-enriched rafts in selective tumor cell apoptosis. J. Exp. Med. 200, 353–365.

Gajate, C., Fonteriz, R.I., Cabaner, C., Álvarez-Noves, G., Álvarez-Rodríguez, Y., Modolell, M., Mollinedo, F., 2000. Intracellular triggering of Fas, independently of FasL, as a new mechanism of antitumor ether lipid-induced apoptosis. Int. J. Cancer 85, 674–682.

Grau, A., Ortiz, A., de Godos, A., Gomez-Fernandez, J.C., 2000. A biophysical study of the interaction of the lipopeptide antibiotic iturin A with aqueous phospholipid bilayers. Arch. Biochem. Biophys. 377, 315–323.

Haugland, H.K., Nygaard, S.J., Tysnes, O.B., 1999. Combined effect of alkyl-lysophospholipid and vincristine on proliferation, migration and invasion in human glioma cell lines in vitro. Anticancer Res. 19, 149–156.

Hayashi, H., Kudo, I., Inoue, K., Nomura, H., Nojima, S., 1985. Macrophage activation by PAF incorporated into dipalmitoylphosphatidylcholine-cholesterol liposomes. J. Biochem. (Tokyo) 97, 1255–1258.

Heimburg, T., Hildebrandt, P., Marsh, D., 1991. Cytochrome c-lipid interactions studied by resonance Raman and ^{31}P NMR spectroscopy. Correlation between the conformational changes of the protein and the lipid bilayer. Biochemistry 30, 9084–9089.

Hochhuth, C., Berkovic, D., Eibl, H., Unger, C., Doenecke, D., 1990. Effects of antineoplastic phospholipids on parameters of cell differentiation in U937 cells. J. Cancer Res. Clin. Oncol. 116, 459–466.

Hoffman, D.R., Thomas, V.L., Snyder, F., 1992. Inhibition of cellular transport systems by alkyl phospholipid analogs in HL-60 human leukemia cells. Biochim. Biophys. Acta 1127, 74–80.

Houlihan, W.J., Lee, M.L., Munder, P.G., Nemecek, G.M., Handley, D.A., Winslow, C.M., Happy, J., Jaeggi, C., 1987. Antitumor activity of SRI 62-834, a cyclic ether analog of ET-18-OCH_3. Lipids 22, 884–890.

Huang, C., Mason, J.T., Stephenson, F.A., Levin, I.W., 1986. Polymorphic phase behavior of platelet-activating factor. Biophys. J. 49, 587–595.

Kosano, H., Takatani, O., 1988. Reduction of epidermal growth factor binding in human breast cancer cell lines by an alkyl-lysophospholipid. Cancer Res. 48, 6033–6036.

Kucera, L.S., Iyer, N., Leake, E., Raben, A., Modest, E.J., Daniel, L.W., Piantadosi, C., 1990. Novel membrane-interactive ether lipid analogs that inhibit infectious HIV-1 production and induce defective virus formation. AIDS Res. Hum. Retroviruses 6, 491–501.

Lohmeyer, M., McNaughton, L., Hunt, S.P., Workman, P., 1994. Stimulation of intracellular free calcium increases by platelet-activating factor in HT29 colon carcinoma cells. Spectrofluorimetric and preliminary spatio-temporal analysis using confocal laser scanning fluorescence imaging microscopy. Biochem. Pharmacol. 47, 975–985.

Lóez-Garcia, F., Villalaín, J., Gómez-Fernández, J.C., Quinn, P.J., 1994. The phase behavior of mixed aqueous dispersions of dipalmitoyl derivatives of phosphatidylcholine and diacylglycerol. Biophys. J. 66, 1991–2004.

Lu, J., Xiao, Y.J., Baudhuin, L.M., Hong, G., Xu, Y., 2002. Role of ether-linked lysophosphatidic acids in ovarian cancer cells. J. Lipid Res. 43, 463–476.

Luzatti, V., 1968. X-Ray diffraction studies of lipid–water systems. In: Chapman, D. (Ed.), Biological Membranes. Academic Press, London, UK, pp. 71–123.

Luzzati, V., Husson, F., 1962. The structure of the liquid-crystalline phases of lipid–water systems. J. Cell. Biol. 12, 207–219.

Marasco Jr., C.J., Piantadosi, C., Meyer, K.L., Morris-Natschke, S., Ishaq, K.S., Small, G.W., Daniel, L.W., 1990. Synthesis and biological activity of novel quaternary ammonium derivatives of alkylglycerols as potent inhibitors of protein kinase C. J. Med. Chem. 33, 985–992.

Maurer, N., Prenner, E., Paltauf, F., Glatter, O., 1994. Phase behavior of the antineoplastic ether lipid 1-*O*-octadecyl-2-*O*-methyl-glycero-3-phosphochloline. Biochim. Biophys. Acta 1192, 167–176.

Mavromoustakos, T., Calogeropoulou, T., Koufaki, M., Kolocouris, A., Daliani, I., Demetzos, C., Meng, Z., Makriyannis, A., Balzarini, J., De Clercq, E., 2001. Ether phospholipid-AZT conjugates possessing anti-HIV and antitumor cell activity. Synthesis, conformational analysis, and study of their thermal effects on membrane bilayers. J. Med. Chem. 44, 1702–1709.

Mavromoustakos, T., Theodoropoulou, E., Yang, D.P., Lin, S.Y., Koufaki, M., Makriyannis, A., 1996. The conformational properties of the antineoplastic ether lipid 1-thiohexadecyl-2-*O*-methyl-sn-glycero-3-phosphocholine. Chem. Phys. Lipids 84, 21–34.

Mollinedo, F., Fernández-Luna, J.L., Gajate, C., Martín-Martín, B., Benito, A., Martínez-Dalmau, R., Modolell, M., 1997. Selective induction of apoptosis in cancer cells by the ether lipid ET-18-OCH_3 (edelfosine): molecular structure requirements, cellular uptake, and protection by Bcl-2 and Bcl-x_L. Cancer Res. 57, 1320–1328.

Mollinedo, F., Martínez-Dalmau, R., Modolell, M., 1993. Early and selective induction of apoptosis in human leukemic cells by the alkyl-lysophospholipid ET-18-OCH_3. Biochem. Biophys. Res. Commun. 192, 603–609.

Munder, P.G., Westphal, O., 1990. Antitumoral and other biomedical activities of synthetic ether lysophospholipids. Chem. Immunol. 49, 206–235.

Nasu, K., Narahara, H., Matsui, N., Kawano, Y., Tanaka, Y., Miyakawa, I., 1999. Platelet-activating factor stimulates cytokine production by human endometrial stromal cells. Mol. Hum. Reprod. 5, 548–553.

Ngwenya, B.Z., Fiavey, N.P., Mogashoa, M.M., 1991. Activation of peritoneal macrophages by orally administered ether analogues of lysophospholipids. Proc. Soc. Exp. Biol. Med. 197, 91–97.

Noseda, A., Godwin, P.L., Modest, E.J., 1988. Effects of antineoplastic ether lipids on model and biological membranes. Biochim. Biophys. Acta 945, 92–100.

Olivier, J.L., Chachaty, C., Quinn, P.J., Wolf, C., 1991. Effects of platelet-activating factor (PAF), lyso-PAF and lysophosphatidylcholine on phosphatidylcholine bilayers, an ESR, ^{31}P NMR and X-ray diffraction study. J. Lipid Mediat. 3, 311–332.

Paltauf, F., 1994. Ether lipids in biomembranes. Chem. Phys. Lipids 74, 101–139.

Paul, W.E., Brown, M., Hornbeck, P., Mizuguchi, J., Ohara, J., Rabin, E., Snapper, C., Tsang, W., 1987. Regulation of B-lymphocyte activation, proliferation, and differentiation. Ann. N.Y. Acad. Sci. 505, 82–89.

Rand, R.P., Fuller, N., Parsegian, V.A., Rau, D.C., 1988. Variation in hydration forces between neutral phospholipids bilayers: evidence for hydration attraction. Biochemistry 27, 771–772.

Ruiter, G.A., Zerp, S.F., Bartelink, H., van Blitterswijk, W.J., Verheij, M., 2003. Anti-cancer alkyl-lysophospholipids inhibit the phosphatidylinositol 3-kinase-Akt/PKB survival pathway. Anticancer Drugs 14, 167–173.

Salgado, J., Villalaín, J., Gómez-Fernández, J.C., 1993. Effects of platelet-activating factor and related lipids on dielaidoylphosphatidylethanolamine by DSC, FTIR and NMR. Biochim. Biophys. Acta 1145, 284–292.

Sánchez-Piñera, P., Aranda, F.J., Micol, V., de Godos, A., Gómez-Fernández, J.C., 1999. Modulation of polymorphic properties of dielaidoylphosphatidylethanolamine by the antineoplastic ether lipid 1-*O*-octadecyl-2-*O*-methyl-glycero-3-phosphocholine. Biochim. Biophys. Acta 1417, 202–210.

Seddon, J.M., 1990. Structure of the inverted hexagonal (H_{II}) phase, and non-lamellar phase transitions of lipids. Biochim. Biophys. Acta 1031, 1–69.

Tardieu, A., Luzatti, V., Reman, F.C., 1973. Structure and polymorphism of the hydrocarbon chains of lipids: a study of lecithin-water phases. J. Mol. Biol. 75, 711–733.

Traikia, M., Warschawski, D.E., Recouvreur, M., Cartaud, J., Devaux, P.F., 2000. Formation of unilamellar vesicles by repetitive freeze-thaw cycles: characterization by electron microscopy and ^{31}P-nuclear magnetic resonance. Eur. Biophys. J. 29, 184–195.

Van der Luit, A.H., Budde, M., Ruurs, P., Verheij, M., van Blitterswijk, W.J., 2002. Alkyl-lysophospholipid accumulates in lipid rafts and induces apoptosis via raft-dependent endocytosis and inhibition of phosphatidylcholine synthesis. J. Biol. Chem. 277, 39541–39547.

Vogler, W.R., Whigham, E., Bennett, W.D., Olson, A.C., 1985. Effect of alkyl-lysophospholipids on phosphatidylcholine biosynthesis in leukemic cell lines. Exp. Hematol. 13, 629–633.

Wagner, F., Rottem, S., Held, H.D., Uhlig, S., Zahringer, U., 2000. Ether lipids in the cell membrane of Mycoplasma fermentans. Eur. J. Biochem. 267, 6276–6286.

Wieder, T., Haase, A., Geilen, C.C., Orfanos, C.E., 1995. The effect of two synthetic phospholipids on cell proliferation and phosphatidylcholine biosynthesis in Madin–Darby canine kidney cells. Lipids 30, 389–393.

Wierenga, P.K., Setroikromo, R., Vellenga, E., Kampinga, H.H., 2000. Purging of acute myeloid leukaemia cells from stem cell grafts by hyperthermia: enhancement of the therapeutic index by the tetrapeptide AcSDKP and the alkyl-lysophospholipid ET-18-OCH(3). Br. J. Haematol. 111, 1145–1152.

Winter, I., Pabst, G., Rappolt, M., Lohner, K., 2001. Refined structure of 1,2-diacyl-P-*O*-ethylphosphatidylcholine bilayer membranes. Chem. Phys. Lipids 112, 137–150.

Xie, X.Q., Moring, J., Makriyannis, A., 1997. Differential scanning calorimetry and small angle X-ray diffraction study of the interaction of (R)-PAF, (R)-ET-18-OMe and (R)-Lyso-PAF with model membranes. Life Sci. 61, 909–923.

Xie, X., Lin, S., Moring, J., Makriyannis, A., 1996. Interdigitation of bilayers from ether lipid analogs: (R)-PAF, (R)-Lyso-PAF and the antineoplastic (R)-ET-18-Ome. Biochim. Biophys. Acta 1283, 111–118.

Zhou, X., Arthur, G., 1997. 1-*O*-Octadecyl-2-*O*-methylglycerophosphocholine inhibits protein kinase C-dependent phosphorylation of endogenous proteins in MCF-7 cells. Biochem. J. 324, 897–902.

Zidovetzki, R., 1997. Role of lipid membrane structure in the mechanism of activation of protein kinase C and phospholipase A2. Curr. Top. Memb. 44, 255–283.